

**3D CEPHALOMETRIC ANALYSIS OF BONE ANCHORED MAXILLARY
PROTRACTION IN GROWING CLASS III PATIENTS**

Jocelyn M. Beville, DDS

A thesis submitted to the faculty of the University of North Carolina at Chapel Hill in partial fulfillment of the requirements for the degree of Master of Science in the School of Dentistry (Orthodontics).

**Chapel Hill
2012**

Approved by:

Lucia Cevitanes, DDS, PhD, MS

Tung Nguyen, DMD, MS

Sylvia A. Frazier-Bowers, DDS, PhD

HongTu Zhu, PhD

©2012
Jocelyn M. Beville
ALL RIGHTS RESERVED

ABSTRACT

JOCELYN M. BEVILLE: 3D Cephalometric Analysis of Bone Anchored Maxillary Protraction in Growing Class III Patients
(Under the direction of Dr. Lucia Cevidanes)

OBJECTIVES: To evaluate the treatment changes produced by bone anchored maxillary protraction (BAMP) on growing Class III patients using 3D cephalometric measurements.

METHODS: CBCT scans were taken before and after treatment on 30 consecutive patients.

Dolphin Imaging software was used to calculate linear, angular, and airway measurements.

The intraclass correlation coefficient was used to test landmark reliability. One-sample t-tests and Pearson correlations were used to evaluate the treatment changes. **RESULTS:** The

maxillary bone orthopedic effects are coupled with forward growth and response to treatment at zygomatic landmarks. Mandibular changes showed statistically significant closure of the mandibular plane angle bilaterally. Although this study sample presented significant

mandibular growth restraint, the airway volume with growth and treatment was significantly increased. **CONCLUSIONS:** Short term assessment of 3D cephalometric changes with

BAMP clearly demonstrated a combination of different skeletal components of midface protraction and mandibular growth restraint without negative effects on airway dimensions.

ACKNOWLEDGEMENTS

In recognition of her time, energy, patience, and guidance with this project, I would like to thank my advisor, Dr. Lucia Cevitanes. She has been a wonderful mentor and friend, and I am honored to have worked with her.

Moreover, I would like to recognize Drs. Tung Nguyen and Sylvia Frazier-Bowers for their extraordinary insight and assistance in bringing this project to fruition.

A special thanks to Dr. Hongtu Zhu and Jiaping Wang for the statistical analysis for this project.

Additionally, I would like to thank the Southern Association of Orthodontists for funding for this research.

Finally, none of this would have been possible without the love and support of my beloved fiancé, family, and friends. I am eternally grateful to each of you.

TABLE OF CONTENTS

LIST OF TABLES.....	vii
LIST OF FIGURES.....	viii
I. LITERATURE REVIEW	1
II. MANUSCRIPT INTRODUCTION.....	10
III. MATERIALS AND METHODS.....	12
IV. RESULTS	15
V. DISCUSSION	18
VI. CONCLUSIONS.....	23
REFERENCES	36

LIST OF TABLES

Table 1. Landmark Definitions	24
Table 2. Linear, Angular, and Airway Measurement Definitions	25
Table 3. Mean Cephalometric Values.....	26
Table 4. Pearson Correlation Values	27

LIST OF FIGURES

Figure 1. Identification of 3D Landmark	28
Figure 2. Example of 3D Linear Measurement	29
Figure 3. Example of 3D Angular Measurement.....	30
Figure 4. Measurement of Airway Volume and Minimum Axial Area.....	31
Figure 5. Soft Tissue Profile Change	32
Figure 6. Boxplot of Mean Linear Change	33
Figure 7. Boxplot of Mean Angular Change	34
Figure 8. Exploratory Cluster Analysis Subgroups	35

I LITERATURE REVIEW

Skeletal Class III Malocclusion

People of European descent have a prevalence of Class III malocclusion ranging between 1-3% in the U.S. population (1). Those of Asian ancestry have an even higher prevalence reported to be as high as 14% in certain countries (2). Many studies have found that Class III malocclusion is a combination of maxillary retrognathia, mandibular prognathia or both. Additionally, negative dentoalveolar compensations have been noted in these patients. One study found that maxillary retrusion was the key component associated with the malocclusion while a much smaller percentage was associated solely with mandibular prognathia (3). Therefore we can surmise that skeletal class III malocclusion is a multi-faceted problem, but a main component of treatment for these patients can be focused on maxillary deficiency.

Current Treatment Options for Class III Patients

Treatment timing for patients with this skeletal discrepancy has proven to be difficult due to the fact that the extent and duration of Class III growth is difficult to reliably predict. One of the most popular treatment choices for the growing patient includes the usage of reverse pull headgear (RPHG) with or without maxillary expansion to protract the maxilla.

Furthermore, treatment with a chin-cup to restrain or redirect mandibular growth is a modality utilized by some clinicians for patients who present with mandibular prognathism. Non-growing patients or growing patients with severe skeletal discrepancies have the option of orthognathic surgery to correct their skeletal discrepancies. Surgical treatment includes a maxillary Lefort I advancement, a mandibular setback, or a combination of the two. Additionally, Class III camouflage is available for those who are non-growing and whose skeletal discrepancy is mild enough to be masked with the extraction of teeth. The presence of crowding in these types of cases complicates the extraction pattern more, and potentially lessens the extent of the camouflage.

Reverse Pull Headgear and Chin Cup Therapy

Treatment with the use of reverse-pull headgear can result in not only skeletal change to the maxilla, but also unwanted dentoalveolar effects on the dentition resulting in proclination of the upper incisors and retroclination of the lower incisors, as well as a clockwise rotation of the mandible (4-8). These undesirable effects must then be corrected during fixed appliance therapy to decompensate the teeth. A down and back rotation of the mandible may be acceptable in a patient with a short anterior face height, but would prove to be an un-esthetic result in a patient with a vertical pattern of growth.

In order for the skeletal changes associated with RPHG to be effective, patient compliance and cooperation during the active phase of treatment is imperative. Patients are required to wear a cumbersome facemask utilizing an intraoral device to which the elastic force is attached for 12-16 hours/day for up to one year. Treatment is generally discontinued

once positive overjet is obtained, however; upon completion of growth, many studies have documented a high potential for dental relapse ranging from 25-33% (9-11). Any treatment that would maximize the amount of skeletal improvement, and limit the amount of dentoalveolar changes during active therapy would be advantageous for these patients. Furthermore, the need for surgical intervention once growth has ceased could potentially be avoided if skeletal growth modification is successful at this stage.

Treatment Timing

Maxillary protraction should be initiated during the peak of maxillary growth in order to obtain the sought after skeletal change (12, 13). One study reported that the peak rate of growth in the maxilla occurred between the ages of 6 and 8 with small increments of growth occurring thereafter until puberty (14). Furthermore, closure of the circum-maxillary sutures occurs at an early age, and this must also be taken into consideration when investigating the best timing of treatment. Wells and Proffit state that clinicians should initiate treatment by the age of 10, but ideally before age 8 (15). Their retrospective study followed 41 patients utilizing protraction facemask with a 5 and 10 year follow-up. They reported that patients treated before 7.92 years of age had less than 20% long term failure rates while those treated after 10.25 years of age had double the amount of failures. Other studies support the earlier treatment timing for maxillary protraction in combination with rapid maxillary expansion to help “loosen” the sutures and aid in displacement of the maxilla (16). One study evaluated three separate age groups (between the ages of 4 and 14) and showed that the 4-7 year old age group displayed the greatest amount of treatment change (17). In support of this finding,

Saadia showed greater skeletal changes in the group of 3-9 year olds vs. the older group of 9-12 year olds (18).

However, Merwin showed that maxillary protraction can be completed at a later stage of development (19). Similar findings were reported by Takada who found successful RPHG and chin cup therapy throughout puberty (20). Cha looked at pre-, peri-, and post-pubertal patients and found that there was no difference in maxillary protraction amongst patients in the pre- and peri-pubertal age groups. In the post-pubertal group, he noted that more dentoalveolar compensation and less skeletal change occurred (21). Baik reported clinical findings in Korean children who underwent maxillary protraction growth modification, and reported no difference in outcomes amongst the three age groups (22). Thus, it is a noteworthy conclusion that maxillary protraction can be effective after age 10, but that more dentoalveolar and less skeletal change might ensue.

Skeletal Anchorage

Through the use of skeletal anchorage, many orthodontic movements are possible. Use of surgical miniplates as skeletal anchorage is frequently reported in the literature, but these uses have been exclusively for dental movement (23-26). In 2003, use of titanium miniplates for maxillary protraction was reported in the literature (27). The bone anchored maxillary protraction protocol included the usage of four Bollard style modified miniplates attached to the zygomatic buttress of the maxilla and between the mandibular canines and lateral incisors. Elastics with a Class III force vector are secured between the upper and lower miniplates by attachments that perforate the mucogingival junction. Patients are instructed to

wear the elastics for twenty-four hours per day, and replace them with new ones once per day. The initial force level begins at 100 g three weeks after miniplate placement and continues up to 250 g of force at the third month of therapy. Active treatment was continued for approximately one year in these 10-13 year old patients. The successful correction of Class III malocclusion has led to widespread interest in exploring the long-term stability of the correction achieved for these patients. Additionally, the success rate with these miniplates for the BAMP protocol is reported to be 97%. Successful stability seems to be dependent upon proper pre-surgical patient counseling, minimally invasive surgery, good post-surgical instructions, and orthodontic follow-up (28).

Two-Dimensional Analysis of Bone Anchored Maxillary Protraction

Treatment with the BAMP protocol has been studied in two dimensions. DeClerck evaluated 21 consecutively treated BAMP patients and matched them to 18 untreated Class III patients based on the severity of Class III malocclusion, age, gender, and duration of observation (29). The study showed that BAMP produced significant orthopedic maxillary protraction as well as mandibular restraint when compared to untreated Class III patients. Furthermore, the authors reported a decrease in the mandibular plane angle, and decompensation of the lower incisors following BAMP treatment. Additionally, the treatment effects of BAMP using thin-plate spline morphometric analysis revealed a marked forward displacement of the maxilla with more moderate favorable changes in the mandible, and no change in the vertical dimension (30).

In order to determine the effectiveness of BAMP vs. conventional Class III therapy, two protocols for maxillary protraction: bone anchors and face mask with rapid expansion were compared (31). The BAMP protocol produced significantly larger maxillary advancement than RME/FM therapy. Vertical changes were shown to be controlled better with BAMP than with RME/FM therapy. Additional findings with BAMP were lack of counterclockwise rotation of the mandible, lack of retroclination of the lower incisors, and a greater improvement in the sagittal intermaxillary relationships.

Given the advantages of 3D over 2D radiographic imaging, a thorough assessment of BAMP treatment outcomes relating to soft tissue, skeletal, dental, and airway changes can be undertaken.

Three-Dimensional Imaging with Cone-Beam Computed Tomography

Traditionally, the 2D image has been the gold standard in orthodontic radiography to assess skeletal treatment changes. Inherent in 2D cephalometry are errors in superimposition, magnification, parallax, and head position. Due to this, it is extremely difficult to make accurate and precise measurements of three dimensional skeletal and dental landmarks on a two dimensional image. The diagnostic image is crucial for diagnosis, treatment planning, and evaluation of treatment changes produced by modalities such as BAMP and RPHG.

In the area of 3D radiography, the use of Cone Beam Computed Tomography (CBCT) has provided clinicians with a more accurate image by which to complete a thorough diagnostic evaluation and the subsequent planning of treatment (32). One of the major benefits of using CBCT is an anatomically precise representation of the craniofacial

structures. Additionally, magnification error does not exist, and the superimposition of structures is not an issue (33). Furthermore, projection error which is common to 2D cephalometry is virtually eliminated with 3D CBCT due to the nature of the orthogonal projection and the correction of any small projection error with the scanner software (34). Another advantage of CBCT imaging is that traditional 2D images can be reconstructed from one 3D scan, thus removing the need for the usual panoramic and cephalometric projections common to orthodontics. These reconstructed images have proven to be comparable to their 2D predecessors (35, 36).

Three-Dimensional Landmark Identification

Observer reliability of 3D cephalometric landmark identification on CBCTs was assessed in a previous study (37). Twelve pre-surgery CBCTs were selected from 159 orthognathic surgery patients. The 30 hard and soft tissue landmarks were selected and criteria were defined for each of these landmarks. Three observers repeated the identification of the landmarks in the sagittal, coronal, and axial slices at three different instances. The results showed overall intra- and inter-observer reliability to be excellent and that 3D landmark identification using CBCT offered consistent and reproducible data if a protocol is followed.

Evaluation of the Oropharyngeal Airway

With the use of the BAMP technique on growing class III patients, an interest in what happens to the upper airway has arisen. The main concern is with possible constriction of the upper airway during mandibular restraint caused by BAMP. Although one study did find an increase in the nasopharyngeal and oropharyngeal after use of RPHG (38), this study was conducted utilizing 2D cephalometric radiology. Several authors concluded that CBCT is an effective method to analyze the airway accurately. Additionally, they found high variability in the airway of patients with similar airways on the lateral headfilm (39-41). This leads us to believe that CBCT is currently the best way to assess any positive or negative changes caused by the BAMP technique.

One study evaluated oropharyngeal differences between children with class I and children with class III malocclusion (42). They found that children with class III malocclusion were subject to having a larger and flatter oropharyngeal airway. Another study evaluated the nasopharyngeal and oropharyngeal airway volume and shape in non-growing patients with different facial patterns (43). This study found that airway shape and volume vary amongst different anteroposterior jaw relationships, whereas airway shape differs with various vertical relationships.

Anatomic limits of the oropharynx and nasopharynx widely vary from study to study. The superior limit of the nasopharynx ranges from the intersection of the line PNS-So (midpoint of the sella-basion line), and the posterior wall of the pharynx to the posterior nasal plane (frontal plane perpendicular to the FH plane passing through PNS (41, 44-46). Several studies agree that the inferior limit of the nasopharynx is the palatal plane (ANS-PNS) extended to the posterior wall of the pharynx (41). The superior limit of the oropharynx is agreed to be the inferior limit of the oropharynx, and several studies agree that the inferior

limit is the horizontal line through the superior point of the epiglottis, although great variability exists among studies about this limit (41).

II INTRODUCTION

Class III malocclusion is one of the most difficult and challenging malocclusions for clinicians to treat due to the unpredictability of the Class III growth pattern – severity and completion of growth are often unknown. Limited and even short-lived success has been achieved with reverse-pull headgear (RPHG) with or without rapid palatal expansion and/or chin cup therapy in the early to mixed dentition (47). The main effects of these treatments were more dentoalveolar than skeletal in nature, with a significant chance of relapse to reverse overjet once mandibular growth had ceased (5, 8, 48-51). The use of maxillary protraction via temporary anchorage devices has increased in recent years to obtain skeletal vs. dentoalveolar changes (52). The bone anchored maxillary protraction (BAMP) technique using miniplates and Class III intermaxillary elastics has proven to be a promising treatment modality for growing Class III patients in the late mixed to permanent dentition (27, 29, 31, 53-58). Skeletal, dental, and soft tissue effects of BAMP have been analyzed in two dimensional cephalometric analyses, and by three-dimensional color maps and surface distances (59). However, the surface distance color maps are very time consuming, and thus far have only been used for research purposes. The development of 3D cephalometry has proposed to be a more accurate method of analysis compared to 2D cephalometry (37, 60-63). A 3D cephalometric analysis could prove to be more user-friendly and less time consuming for clinicians to operate versus other surface-based methods of 3D analysis. The purpose of this study was to evaluate and characterize the treatment effects of BAMP

utilizing a novel 3D cephalometric analysis. The specific aims were to evaluate 1) skeletal changes in the maxilla 2) dental and soft tissue changes, and 3) whether or not growth of the oropharyngeal airway space was restricted with BAMP treatment.

III MATERIALS AND METHODS

Subjects

This prospective sample consisted of 30 consecutively treated patients (16 females and 14 males) with an age range of 9-13 years (mean 11.1 ± 1.1 years). All patients were of Caucasian decent, skeletal Class III (Wits appraisal of -1mm or greater) with overjet or incisor end-to-end relationship, and had a skeletal maturation stage of CVM1-3 at T1 (64).

BAMP Protocol

All patients had 4 miniplates placed on the right and left infrazygomatic crest of the maxillary buttress and between the mandibular left and right lateral incisor and canine. Each of the miniplates was secured to bone with 2 or 3 screws. Extensions of the miniplates perforated the attached gingiva near the mucogingival junction. Three weeks after surgery, the miniplates were loaded. Class III elastics were applied with an initial force of 150 grams/side, and increased to a final force level of 250 grams/side. The patients were instructed to wear the elastics 24 hrs/day. In some cases, a removable bite plate was used to eliminate occlusal interferences in the incisor area (27).

3D Cephalometric Analysis

CBCT scans were acquired in DICOM format using an iCAT machine (Imaging Sciences International, Hartsfield, PA) with a 40-second scan and a 16x22-cm field of view. The T1 (immediately after placement of the miniplates) and T2 (mean 1.1 years \pm 1 month) cone beam scans were analyzed for these patients treated with the BAMP protocol. The cephalometric measurements selected were based on a previously described reference system traced through stable structures, and have been proven to be reliable (37). The 3D landmarks are defined on Table 1, and were identified for each time point (Figure 1). The AWS (anterior wall of sella) and CG (crista galli) landmarks were included in this study instead of Sella and Nasion. Sella and Nasion have historically been used in 2D cephalometry not because of their biologic significance, but for their easiness of identification. The use of AWS and CG landmarks in this study aimed to select stable landmarks as a reference relative to the cranial base. The ossification of crista galli and the anterior tip of the endocranial surface of the cribiform plate are almost complete at 2 years of age, and for this reason, the top of crista galli has been described as a stable anterior endocranial anatomic landmark in CT studies (65). Selection and definition of anatomic measurements (Table 2 and Figures 2 and 3) aimed to describe maxillary and mandibular skeletal and dental changes, facial convexity, and airway measurements. The boundaries of the airway volume were determined superiorly by the extension of the palatal plane (PNS-ANS) to the posterior wall of the pharynx parallel to the posterior border of the vomer, and inferiorly by a horizontal plane from the superior surface of the epiglottis to the top of the 2nd cervical vertebrae. All 3D linear, angular, area, and volume measurements were performed at each time point using Dolphin Imaging 11.5 (Dolphin Imaging and Management Systems, Chatsworth, CA).

Landmark Reliability

The intraclass correlation analysis was used to assess the reliability of the landmark identification. Ten randomly selected T1 CBCT's that were digitized on three occasions at one week intervals by the same observer (J.B.). The validity and reliability of the method as determined by previous studies proved to be acceptable (62).

Statistical Analysis

Descriptive statistics were calculated for all measures at T1 and T2. T1 and T2 changes were assessed using mean, standard deviation, range, 95% confidence interval, and Pearson correlation coefficient. The power for this study was 81% with a two-sided significance level of 0.05, a standard deviation of 0.9 mm, and a sample size of 30 by using PROC POWER in SAS v.9.1 (SAS Institute Inc., Cary, NC). An exploratory cluster analysis, with the sample size of 30 and based on landmark coordinates at T1, was used to test variability of individual 3D facial morphology. This analysis proceeded by a series of steps in which each subject, characterized by the array of 3D landmarks, was progressively grouped together into a series of larger clusters. The Ward's linkage and the Euclidean distance metric were used to cluster the subjects (66). Individual subjects, therefore, were clustered together only if their component dimensions added the least to the variability within the group.

IV RESULTS

The Intraclass correlation coefficient (ICC) ranged from 0.88 to 0.99 for the intra-observer reliability implying high intra-observer consistency for all 3D cephalometric measurements

Maxillary Skeletal Changes

The maxillary 3D linear measurements shown in Table 3 and Figures 5-6 revealed a statistically significant ($p < 0.00$) increase in anterior-posterior dimensions of the maxilla, as measured mid-sagittally from the posterior nasal spine (PNS) or bilaterally from the right and left tuberosity to the anterior nasal spine (ANS) anteriorly. Significant forward growth and response to treatment was also measured from the anterior wall of sella to both ANS and to zygomatic landmarks bilaterally.

Mandibular Skeletal Changes

There was a statistically significant decrease in the rCo-rGo-Me and lCo-lGo-Me angles, with a 95% confidence interval of -3.06° to -0.4° , and -2.8° to -0.66° , $p = 0.01$ and $p < 0.00$, for right and left sides respectively. Corpus length and total mandibular length

increased bilaterally with growth and treatment ($p < 0.00$). Both the ramus height and the total anterior face height were also significantly increased at T2 (Table 3, Figures 5-6).

Facial Convexity

There were statistically significant decreases in angular measurements for both hard tissue (CG-A-Pg) and soft tissue (Subn-UL-LL) respectively with a mean of $-4.42^\circ \pm 3.24^\circ$ and $-7.18^\circ \pm 10.85^\circ$ (Table 3).

Dentoalveolar Changes

No statistically significant dental compensations were observed for the upper and lower incisors, as measured by the T2 – T1 changes for PNS-ANS-rUIE and rGo-Me-rLIE and lGo-Me-lLIE (Table 3, Figures 5-6).

Airway Changes

Airway volume increased significantly an average of $1411.59 \pm 2996.46 \text{ mm}^3$. The area in the most constricted section of the airway increased slightly on average $13.11 \pm 53.81 \text{ mm}^2$, but this increase was not statistically different at T2 compared to T1.

Correlations between Changes in Different Anatomic Regions (Table 4)

Changes in AWS-CG-A and AWS-CG-B were highly positively correlated with each other ($p < 0.00$) and with rCo-rGo-Me, lCo-lGo-Me, PNS-ANS-rUIE, rGo-Me-rLIE, and lGo-Me-rLIE.

The minimum axial area of the airway was significantly positively correlated with the airway volume ($p < 0.00$). The increase in airway volume was highly correlated with the amount of protraction and growth response measured at AWS-rZS and AWS-lZS.

The results of the exploratory cluster analysis identified 4 subgroups of craniofacial morphology at T1 that are shown in Figure 4.

V DISCUSSION

This study expanded the sample evaluated in prior 3D overall facial superimposition studies of BAMP (57, 58) and presented a more clinician-friendly method of assessment of treatment outcomes.

Our results corroborated previous 3D BAMP assessments demonstrating favorable skeletal, dental, soft tissue, and airway treatment changes for the correction of maxillary deficiency and/or mandibular prognathism (57, 58).

The use of CBCT in this study allowed for a three dimensional tracing with no bias of magnification and parallax as occurs in 2D cephalometry. The measurements taken were true 3D linear and angular measurements. The 3D cephalometric analysis described in this study does not require construction of surface models, voxels, or surface-based 3D superimpositions and computation of closest corresponding surface distances (67). The proposed 3D landmarks' reliability has been previously tested (37), and the addition of new landmarks in the search for 3D landmarks with greater biological meaning has shown very good to excellent reliability ($ICC > 0.9$).

Three dimensional data on untreated controls are not currently available. For this reason, indirect discussions in this study refer to previously reported 2D cephalometric findings of

growth in Class III untreated controls (29) or treatment response with facemask (56). Two dimensional cephalometric data showed 4 mm of maxillary improvement with bone-anchored maxillary protraction treatment, measured at A-point, when compared with the untreated controls (29).

The skeletal midface changes observed in this study showed an average net maxillary growth of 2.2 mm measured midsagittally from PNS or bilaterally from the right and left tuberosity posteriorly to ANS anteriorly. Additionally, there was a significant average 2.2 mm displacement of the right and left tuberosities relative to the anterior wall of sella, and an average increase of 2.74 mm in the distance AWS-ANS indicating a forward direction of growth and response to treatment of the maxilla. The previous 3D assessment of bone anchored maxillary protraction treatment using closest point surface distances reported 3.73 mm of maxillary protraction (57). Those findings cannot be directly compared to our findings because they refer to maximum closest point displacement of the maxilla relative to the anterior cranial base superimposition (overall facial change). The findings reported in the present study refer to 3D inter-landmark distances and angles at specific locations. Our findings of significant changes in the zygomatico-maxillary suture landmarks and all maxillary landmarks relative to the anterior cranial base corroborate the findings reported with 3D color maps and indicate that the midface was displaced anteriorly as a unit (57).

The A-P positions of the chin relative to the cranial base in this study did not present significant changes and was maintained with growth and response to BAMP treatment. Condylion-gnathion bilateral linear measurements showed less than a 2 mm increase, while a

2D cephalometric study reported that a 3 mm increase in mandibular length per year may be expected in an untreated Class III population of the same age as the sample in our study (13).

The present 3D cephalometry study showed slight but statistically significant closure of the gonial angle bilaterally, with counterclockwise rotation of the mandibular plane. These findings corroborate the previous study of 2D outcomes, while in untreated Class III subjects a clockwise rotation of the mandibular plane angle has been observed (29).

Anterio-posterior changes in the position of the maxilla relative to the cranial base were significantly correlated to changes in the chin position. Both the maxillary and mandibular positions relative to the cranial base at the end of treatment with BAMP were significantly correlated to the amount of closure of the gonial angle bilaterally, and changes in the upper and lower incisor inclinations. The 3D angular measurements of upper and lower incisor inclination relative to the mandibular planes bilaterally showed no significant changes with growth and treatment, which differs from 2D findings of treatment with either facemask (56) or chin cup (68).

Significant changes in facial convexity were observed for both hard and soft tissues with -4.42° and -7.18° changes for CG-A-Pg and Subn-UL-LL, respectively. The soft tissue changes with BAMP reflect truly remarkable changes in the perioral musculature, as measured by the angular change in soft tissue facial convexity in this study with a 95% confidence interval of -12.5° to -3.63° . One patient presented with 42.1° of change in the Subn-UL-LL, and the use of intermaxillary elastics was discontinued at the T2 CBCT (Figure 4). These findings were in agreement with the results described by Nguyen where the

superimposed color maps display forward movement of the upper lip, and often backwards movement of the lower lip at the completion of treatment (57).

Interestingly, this study has shown that no adverse effects on the size of the airway occurred with BAMP treatment despite its mandibular restraint effects. In fact, the airway volume was significantly increased and was positively correlated with changes in the anterior wall of sella to the zygomatic sutures as well as minimum axial area of the airway. Minimum axial area of the airway also correlated with AWS-ANS changes. These findings indicate that the maxillary protraction with BAMP may enlarge the upper oropharyngeal airway. Airway assessments in CBCT need to be interpreted carefully, as definition of airway boundaries, respiration phase, and head posture are critical for these assessments. The oral maxillofacial radiologist responsible for all image acquisitions in this study strived to control head posture and position.

The factors that affect the marked individual variability observed in the response to BAMP treatment in this study remain important clinical questions. The inter-patient variability in response to treatment could not be explained by factors such as compliance, stage of pubertal growth, loss or loosening of bone anchors, or discontinuation of treatment because 1) cooperation was not a problem in this sample, as only intra-oral elastics had to be worn; 2) There were no broken appliances or problems with appointments in the sample; 3) oral hygiene had no impact on inflammation around bone anchor sites; 4) all patients completed their treatment and continued their inter-maxillary traction for at least one year as originally determined by the protocol; 5) all patients were treated during their pubertal growth spurt.

The sample size of 30 subjects allowed us to perform an exploratory cluster analysis to evaluate the variability of the craniofacial morphology as described by the 3D landmarks in this study; however, the sample size in each cluster is too small to evaluate differences in response to treatment.

The results reported in this study refer to findings at the end of active treatment. While these short term results are encouraging, future long-term studies are needed to clarify post-pubertal stability, particularly for cases who presented with marked mandibular rotations in response to treatment.

VI CONCLUSIONS

The findings of this three dimensional analysis of BAMP in growing Class III patients revealed:

- 1) Marked forward growth of the maxilla and zygomas.
- 2) Control of mandibular growth with counterclockwise rotation of the angle between the mandibular ramus and corpus.
- 3) Improvement of both hard and soft tissue convexity.
- 4) No restriction of the posterior airway space as a result of mandibular restraint, and a significant increase in airway volume.

VII. TABLES

Table 1. Landmark Definitions

Landmark name	Anatomic region	Lateral view	Axial view	Antero-posterior view
1 - Anterior Wall of Sella Turcica (AWS)	Anterior wall of the pituitary fossa of the sphenoidal bone	Middle point of the anteroposterior width of the fossa	Middle point of the anteroposterior and lateral width of the fossa	Middle point of the lateral width of the fossa in the antero-posterior slice determined by the lateral and axial views
2 - Crista Galli (N)	Triangular midline process of the ethmoid bone extending upward from the cribriform plate	Superior-most point	Middle-anterior-most point on the anterior contour of the crista galli	Middle-superior-most point of the crista galli seen as a vertically elongated, diamond-shaped radiopacity, appearing between the orbital outlines endocranial surface
3 - A point (A)	Premaxilla	Posterior-most point on the curve of the maxilla between the anterior nasal spine and supradentale	Middle-anterior-most point on the tip of the premaxilla	Middle point in the antero-posterior slice determined by the lateral and axial views
4 - Anterior Nasal Spine (ANS)	sharp anterosuperior projection at the anterior extremity of the maxilla	Point on the median antero-superior tip	Anterior-most point	Middle point in the antero-posterior slice determined by the lateral and axial views
5 - Posterior Nasal Spine (PNS)	sharp posterior extremity of the bony hard palate	mid-point between the inferior and the superior surfaces of the bony hard palate (nasal floor) in the midsagittal plane	Median posterior-most point in the palatal surface	Middle point in the antero-posterior slice determined by the lateral and axial views
6 - Right Orbitale (rOr)	Latero-inferior contour of the right orbit	Anterior-superior-most point on the edge between the internal and external contours	Anterior-most point	Latero-inferior most point
7 - Left Orbitale (lOr)	Latero-inferior contour of the left orbit	Anterior-superior-most point on the edge between the internal and external contours	Anterior-most point	Latero-inferior most point
8 - Right Tuberosity (rTb)	Distal contour of the right maxillary tuberosity	Posterior-inferior-most point	Posterior-most point	Inferior-most point
9 - Left Tuberosity (lTb)	Distal contour of the left maxillary tuberosity	Posterior-inferior-most point	Posterior-most point	Inferior-most point
10 - Right Zygomatic Suture (rZS)	Zygomaticomaxillary suture	Anterior-inferior-most point	Anterior-most point	Lateral-inferior-most point
11 - Left Zygomatic Suture (lZS)	Zygomaticomaxillary suture	Anterior-inferior-most point	Anterior-most point	Lateral-inferior-most point
12 - Right Upper Incisal Edge (rUIE)	Incisal tip of right upper central incisor	Inferior-most point	Middle point of the mesiodistal and buccolingual width	Middle point of the mesiodistal width
13 - B point (B)	Anterior surface of the mandibular symphysis	Posterior-most point	Middle-anterior-most point on the anterior contour	Middle point in the antero-posterior slice determined by the lateral and axial views
14 - Pogonion (Pg)	Contour of the bony chin	Anterior-most point	Middle-anterior-most point on the anterior contour	Middle point in the antero-posterior slice determined by the lateral and axial views
15 - Gnathion (Gn)	Contour of the bony chin	Anterior-inferior-most point	Middle-anterior-inferior-most point	Middle-inferior-most point
16 - Menton (Me)	Lower border of the mandible	Inferior-most point	Middle-inferior-most point	Inferior-most point
17 - Right mandibular Gonion (rGo)	Angle of the right mandibular body	Middle point along the angle	Posterior-most point	Inferior-most point
18 - Left mandibular gonion (lGo)	Angle of the left mandibular body	Middle point along the angle	Posterior-most point	Inferior-most point
19 - Right Condylion (rCo)	Right condyle	Superior-most point	Middle point in the axial slice level determined by the lateral and antero-posterior views	Middle Superior-most point
20 - Left Condylion (lCo)	Left condyle	Superior-most point	Middle point in the axial slice level determined by the lateral and antero-posterior views	Middle Superior-most point
21 - Right Lower Incisal Edge (rLIE)	Incisal tip of right lower central incisor	Superior-most point	Middle point of the mesiodistal and buccolingual width	Middle point of the mesiodistal width
22 - Subnasale	Base of the nose columella	Inferior-most point in the soft tissue contour of the base of the nose columella	Middle point of the columella at the labial junction	Middle point of the columella at the labial junction

Table 2. Linear, Angular, and Airway Definitions

Measurements		Definition	Measurement
Maxilla/ Zigoma	rTb - ANS	Right Tuberosity (rTb) – Anterior Nasal Spine (ANS)	Right maxillary antero-posterior dimension
	lTb - ANS	Left Tuberosity (lTb) – Anterior Nasal Spine (ANS)	Left maxillary antero-posterior dimension
	PNS - ANS	Posterior Nasal Spine (PNS) – Anterior Nasal Spine (ANS)	Midsagittal maxillary antero-posterior dimension
	AWS - ANS	Anterior Wall of Sella (AWS) – Anterior Nasal Spine (ANS)	Distance of anterior nasal spine to anterior wall of sella
	AWS - rZS	Anterior Wall of Sella (AWS) – Right Zygomatic Suture (rZS)	Distance of right zygomatic suture to anterior wall of sella
	AWS - lZS	Anterior Wall of Sella (AWS) – Left Zygomatic Suture (lZS)	Distance of left zygomatic suture to anterior wall of sella
	AWS - CG - A	Anterior Wall of Sella (AWS) – Crista Galli (CG) – A Point (A)	Anteroposterior position of the maxilla relative to cranial base
Mandible	rGo - Me	Right Mandibular Gonion (rGo) – Menton (Me)	Mandibular body length on the right side
	lGo - Me	Left Mandibular Gonion (lGo) – Menton (Me)	Mandibular body length on the left side
	rCo - rGo	Right Condylion (rCo) – Right Mandibular Gonion (rGo)	Posterior facial height on the right side
	lCo - lGo	Left Condylion (lCo) – Left Mandibular Gonion (lGo)	Posterior facial height on the left side
	ANS - Me	Anterior Nasal Spine (ANS) – Menton (Me)	Anterior facial height
	rCo - Gn	Right Condylion (rCo) – Gnathion (Gn)	Total mandibular length on the right side
	lCo - Gn	Left Condylion (lCo) – Gnathion (Gn)	Total mandibular length on the left side
	AWS - CG - B	Anterior Wall of Sella (AWS) – Crista Galli (CG) – B Point (B)	Anteroposterior position of the mandible relative to cranial base
	rCo - rGo - Me	Right Condylion (rCo) – Right Gonion (rGo) – Menton (Me)	Gonial angle on the right side (mandibular ramus/corpus angle)
	lCo - lGo - Me	Left Condylion (lCo) – Left Gonion (lGo) – Menton (Me)	Gonial angle on the left side (mandibular ramus/corpus angle)
Facial Convexity	CG - A - Pg	Crista Galli (CG) – A Point (A) – Pogonion (Pg)	Convexity angle
	Subn - UL - LL	Subnasale (Subn) – Upper Lip (UL) – Lower Lip (LL)	Soft tissue convexity
Dental	PNS - ANS - rUIE	Posterior Nasal Spine (PNS) – Anterior Nasal Spine (ANS) – Right Upper Incisal Edge (rUIE)	Inclination of the upper incisor to the palatal plane
	rGo - Me - rLIE	Right Gonion (rGo) – Menton (Me) – Right Lower Incisal Edge (rLIE)	Inclination of the right lower incisor to the right mandibular plane
	lGo - Me - lLIE	Left Gonion (lGo) – Menton (Me) – Left Lower Incisal Edge (lLIE)	Inclination of the left lower incisor to the left mandibular plane
Airway	Airway Volume (mm ³)	Superior limit: from the palatal plane (ANS-PNS) extended to the posterior wall of the pharynx. Inferior limit: from a horizontal line from the superior point of the epiglottis to the 2 nd cervical vertebrae	Volume of the pharynx
	Minimum Axial Area (mm ²)	Smallest area in an axial cross-section of the pharynx.	Most constricted area in the pharynx

Table 3. Mean, standard deviation, range, and confidence interval for linear, angular, and airway changes. The level of significance was set at $p < 0.05$.

Measurements		Mean	SD	Range	T2-T1 >0:pval	95% CI
Maxilla/ Zigoma	rTb - ANS	2.22	2.23	(-2.5, 7.4)	0.00*	(1.39,3.06)
	ITb - ANS	2.3	1.77	(-0.7, 6.7)	0.00*	(1.64,2.97)
	PNS - ANS	2.2	1.72	(-1.0, 6.4)	0.00*	(1.55,2.84)
	AWS - ANS	2.74	1.75	(-1.0, 5.9)	0.00*	(2.08,3.39)
	AWS - rZS	2.61	1.93	(-0.3, 7.2)	0.00*	(1.89,3.33)
	AWS - IZS	1.87	2.01	(-0.6, 8.1)	0.00*	(1.12,2.62)
	AWS - CG - A	1.35	8.19	(-39.0,10.5)	0.37	(-1.71,4.41)
Mandible	rGo - Me	1.71	1.98	(-2.4, 6.6)	0.00*	(0.97,2.44)
	IGo - Me	2.15	2.5	(-0.8, 9.3)	0.00*	(1.22,3.09)
	rCo - rGo	1.51	1.66	(-3.5, 5.1)	0.00*	(0.89,2.13)
	ICo - IGo	1.8	1.96	(-0.8, 8.4)	0.00*	(1.07,2.53)
	ANS - Me	1.09	1.73	(-1.4, 5.5)	0.00*	(0.45,1.74)
	rCo - Gn	1.79	1.13	(-0.4, 3.8)	0.00*	(1.37,2.22)
	ICo - Gn	1.49	1.53	(-0.8, 6.3)	0.00*	(0.92,2.06)
	AWS - CG - B	-0.27	8.5	(-42.1, 9.1)	0.86	(-3.44,2.91)
	rCo - rGo - Me	-1.73	3.56	(-13.1, 4.2)	0.01*	(-3.06,-0.4)
	ICo - IGo - Me	-1.73	2.87	(-10.5, 1.7)	0.00*	(-2.8,-0.66)
Facial Convexity	CG - A - Pg	-4.46	3.19	(-10.4, 3.5)	0.00*	(-5.65,-3.3)
	Subn - UL - LL	-7.84	11.27	(-42.1,12.7)	0.00*	(-12.05,-3.63)
Dental	PNS - ANS - rUIE	0.96	5.38	(-15.4,13.8)	0.34	(-1.05,2.97)
	rGo - Me - rLIE	0.94	4.16	(-11.1, 7.8)	0.22	(-0.61,2.50)
	IGo - Me - rLIE	0.93	4.53	(-16.0, 8.5)	0.27	(-0.76,2.62)
Airway	Airway Volume (mm3)	1411.59	2996.46	(-3726.5,8495.4)	0.02*	(292.69,2530.49)
	Minimum Axial Area (mm2)	13.11	53.81	(-99.2,122.5)	0.19	(-6.98,33.21)

Table 4. Pearson correlation table evaluating correlations between all measurements.

Measures	rGo-Me	lGo-Me	ANS-Me	rCo-Gn	lCo-Gn	rCo-rGo	lCo-rGo	rTb-ANS	lTb-ANS	PNS-ANS	AWS-ANS	AWS-IZS	AWS-rZS	AWS-CG-A	AWS-CG-B	rCo-Me	lCo-Me	CG-A-Pg	Subn-UL-LL	PNS-ANS-rLIE	rGo-Me-rLIE	lGo-Me-rLIE	Airway Volume	Minimum Axial Area
rGo-Me		0.03	0.03	0.9	0.83	0.02	0.35	0.65	0.95	0.55	0.39	0.81	0.41	0.93	0.98	0.5	0.45	0.47	0.98	0.86	0.1	0.83	0.9	0.29
lGo-Me	0.41		0.87	0.36	0.85	0.02	0.01	0.6	0.61	0.72	0.41	0.3	0.82	0.56	0.48	0.83	0.01	0.61	0.73	0.8	0.67	0.92	0.71	0.84
ANS-Me	0.41	0.03		0.04	0.32	0.52	0.61	0.83	0.5	0.76	0.22	0.8	0.92	0.58	0.59	0.86	0.28	0.62	0.4	0.92	0.03	0.26	0.51	0.29
rCo-Gn	0.02	-0.17	0.39		0.76	0.36	0.8	0.62	0.58	0.83	0.81	0.15	0.02	0.24	0.22	0.28	0.58	0.8	0.4	0.33	0.21	0.17	0.19	0.17
lCo-Gn	-0.04	-0.04	0.19	0.06		0.34	0.02	0.44	0.02	0.08	0.18	0.49	0.59	0.55	0.49	0.63	0.49	0.4	0.04	0.9	0.17	0.36	0.54	0.21
rCo-rGo	-0.42	-0.41	0.12	0.17	0.18		0.06	0.87	0.28	0.12	0.16	0.16	0.25	0.2	0.25	0.91	0.39	0.76	0.53	0.96	0.28	0.14	0.21	0.79
lCo-lGo	-0.18	-0.5	0.1	0.05	0.41	0.35		0.99	0.83	0.64	0.86	0.38	0.95	0.63	0.6	0.74	0.02	0.81	0.97	0.93	0.69	0.59	0.98	0.7
rTb-ANS	-0.09	0.1	0.04	-0.09	0.15	0.03	0		0.01	0.12	0	0.56	0.1	0.06	0.02	0.7	0.04	0.01	0.06	0	0.4	0.4	0.35	0.23
lTb-ANS	-0.01	0.1	0.13	-0.11	0.41	0.2	0.04	0.44		0	0.04	0.77	0.21	0.64	0.66	0.8	0.54	0.21	0.04	0.37	0.87	0.69	0.63	0.38
PNS-ANS	-0.11	-0.07	-0.06	0.04	0.33	0.29	-0.09	0.29	0.69		0.03	0.08	0.27	0.31	0.35	0.13	0.11	0.18	0.08	0.35	0.37	0.48	0.2	0.17
AWS-ANS	-0.16	-0.16	0.23	0.04	0.25	0.27	0.03	0.58	0.38	0.39		0.06	0	0.71	0.57	0.18	0.69	0.01	0.2	0.06	0.4	0.95	0.12	0.01
AWS-rZS	0.05	-0.19	-0.05	0.27	0.13	0.26	0.17	0.11	0.06	0.33	0.35		0.01	0.75	0.69	0.02	0.92	0.25	0.8	0.73	0.82	0.44	0.03	0.14
AWS-IZS	-0.16	0.04	-0.02	0.41	0.1	0.22	-0.01	0.31	0.23	0.21	0.53	0.45		0.89	0.83	0.06	0.75	0.02	0.34	0.87	0.55	0.78	0	0
AWS-CG-A	0.02	-0.11	-0.1	-0.22	-0.11	-0.24	0.09	-0.34	0.09	-0.19	-0.07	-0.06	0.03		0	0	0	0.39	0.06	0	0	0	0.56	0.2
AWS-CG-B	0	-0.13	-0.1	-0.23	-0.13	-0.22	0.1	-0.41	0.08	-0.18	-0.11	-0.08	-0.04	0.98		0	0	0.93	0.04	0	0	0	0.42	0.18
rCo-rGo-Me	-0.13	-0.04	0.03	-0.2	-0.09	-0.02	0.06	-0.07	0.05	-0.28	-0.25	-0.41	-0.35	0.56	0.55		0.03	0.92	0.1	0.01	0.2	0.09	0.23	0.02
lCo-lGo-Me	-0.14	-0.44	0.2	0.1	-0.13	0.16	0.43	-0.37	-0.12	-0.3	-0.08	0.02	-0.06	0.52	0.59	0.4		0.01	0.13	0.16	0.43	0.08	0.25	0.1
CG-A-Pg	-0.14	-0.1	0.09	0.05	-0.16	0.06	0.05	-0.44	-0.24	-0.25	-0.44	-0.22	-0.42	-0.16	-0.02	0.02	0.45		0.2	0.65	0.69	0.94	0.11	0.26
Subn-UL-LL	0	0.07	-0.16	-0.16	-0.37	-0.12	0.01	-0.34	-0.37	-0.32	-0.24	-0.05	-0.18	0.35	0.38	0.31	0.29	0.24		0.12	0.15	0.07	0.63	0.08
PNS-ANS-rLIE	-0.03	-0.05	-0.02	0.18	0.02	0.01	0.02	-0.5	-0.17	-0.18	-0.35	0.07	-0.03	0.56	0.55	0.48	0.26	-0.09	0.29		0.02	0.05	0.54	0.33
rGo-Me-rLIE	-0.3	-0.08	-0.4	-0.24	-0.26	-0.2	-0.07	-0.16	0.03	-0.17	-0.16	0.04	0.11	0.61	0.58	0.24	0.15	-0.07	0.27	0.42		0	0.74	0.99
lGo-Me-rLIE	0.04	-0.02	-0.21	-0.25	-0.17	-0.27	-0.1	-0.16	0.07	-0.13	-0.01	0.15	0.05	0.71	0.72	0.32	0.32	-0.01	0.33	0.36	0.65		0.81	0.72
Airway Volume	-0.02	-0.07	-0.13	0.25	0.12	0.23	0.01	0.18	0.09	0.24	0.29	0.4	0.55	-0.11	-0.15	-0.23	-0.22	-0.3	-0.09	0.12	0.06	0.05		0
Minimum Axial Area	-0.2	-0.04	-0.2	0.26	0.24	0.05	-0.07	0.23	0.17	0.26	0.45	0.28	0.54	-0.24	-0.25	-0.41	-0.3	-0.21	-0.32	-0.18	0	-0.07	0.73	

VIII. FIGURES

Figure 1. Identification of ANS landmark in the 3 planes of space. The 3D rendering is included for visualization purposes only.

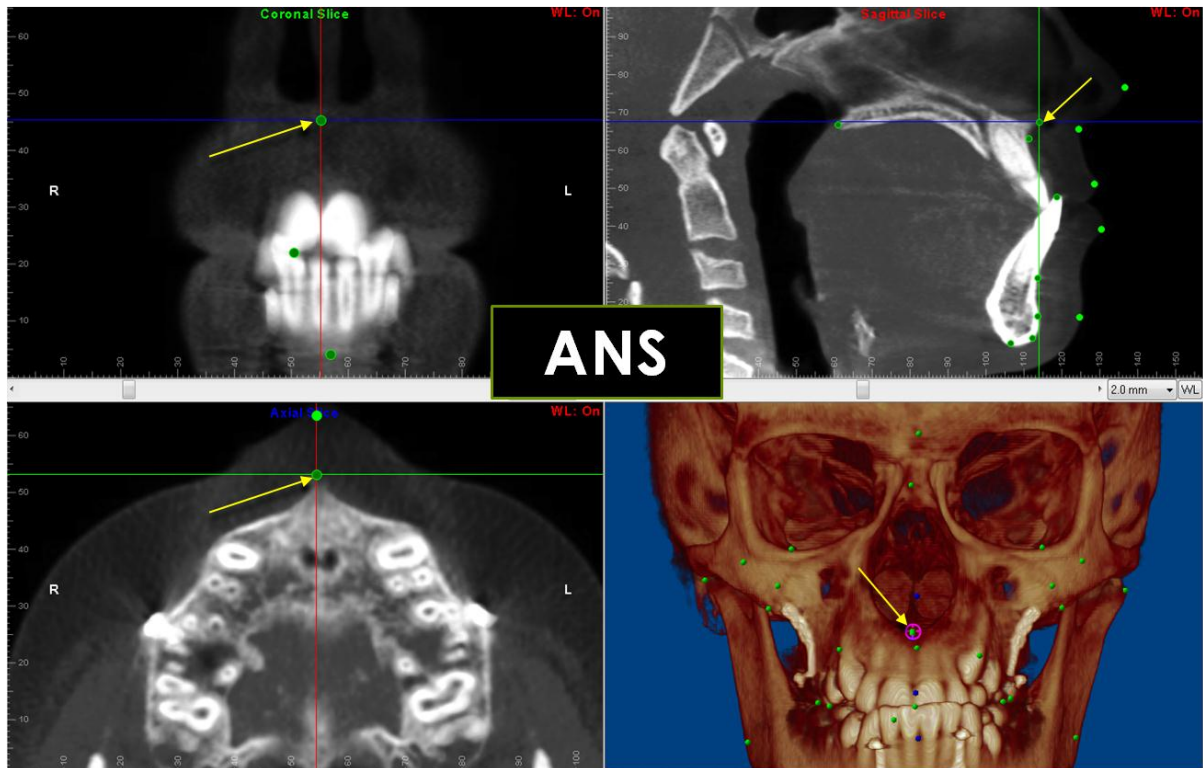


Figure 2. Three-dimensional linear measurement example (AWS-ANS) displayed in the 3D rendering.

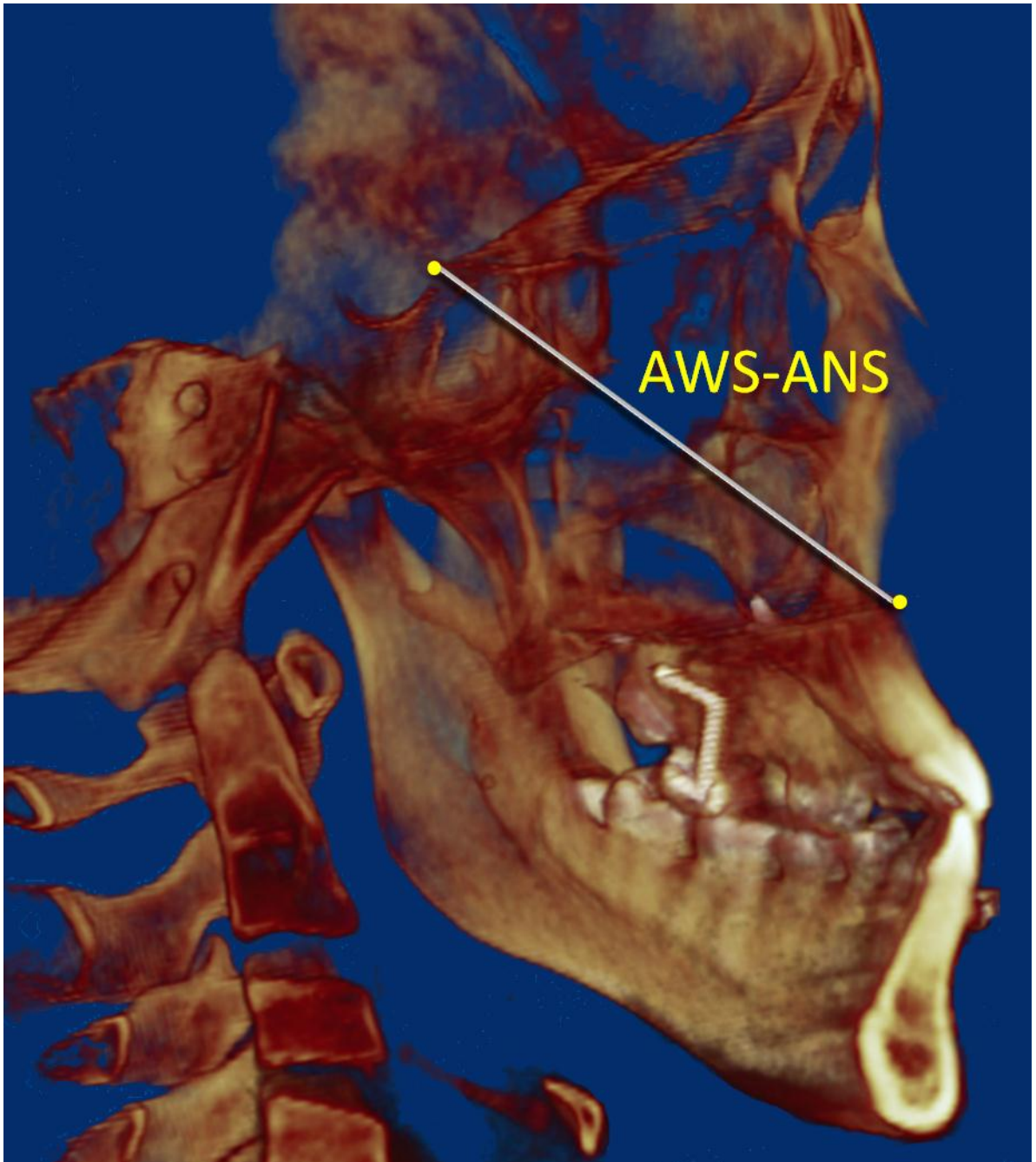


Figure 3. Three-dimensional angular measurement example (rCo-rGo-Me) displayed in the 3D rendering.

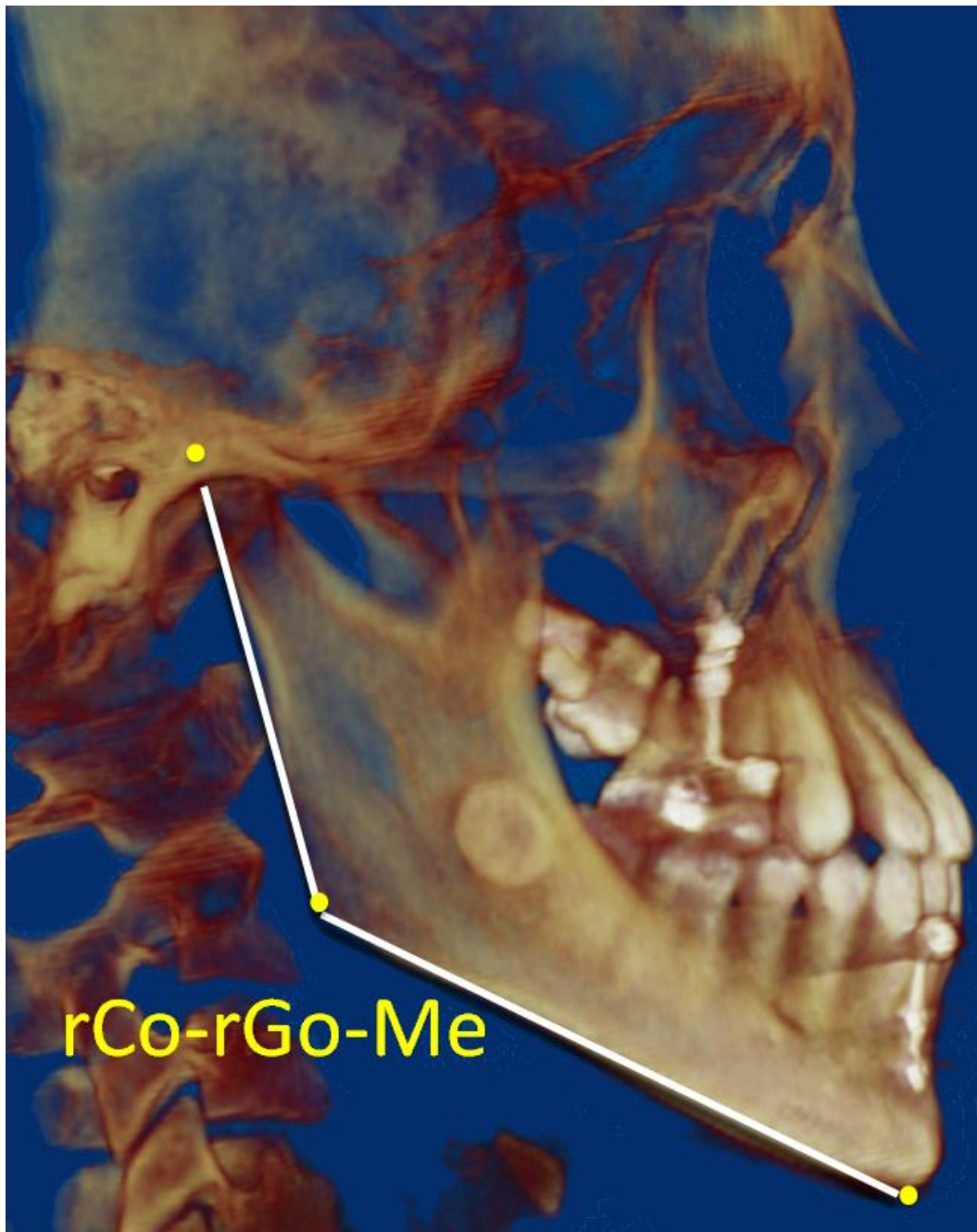


Figure 4. Measurement of airway volume and minimum axial shown in a patient at the end of active treatment.

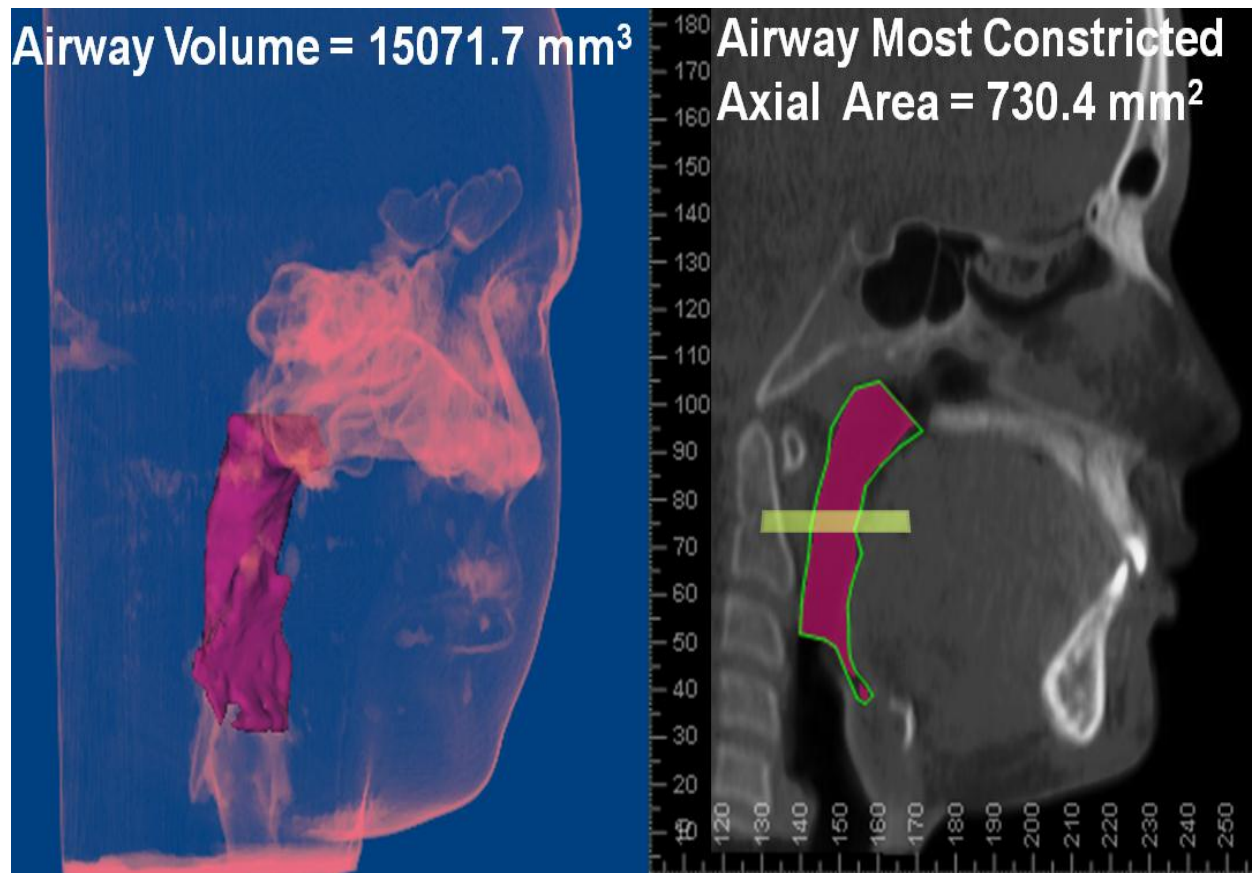


Figure 5. Remarkable changes in soft tissue profile for one patient with 42.1° of changes in the Subn-UL-LL angle. This result is an outlier compared to the response of all other patients, but the improvement of soft tissue profile as measured by changes in the Subn-UL-LL angle had a 95% confidence interval of -12.5° to -3.63° changes.

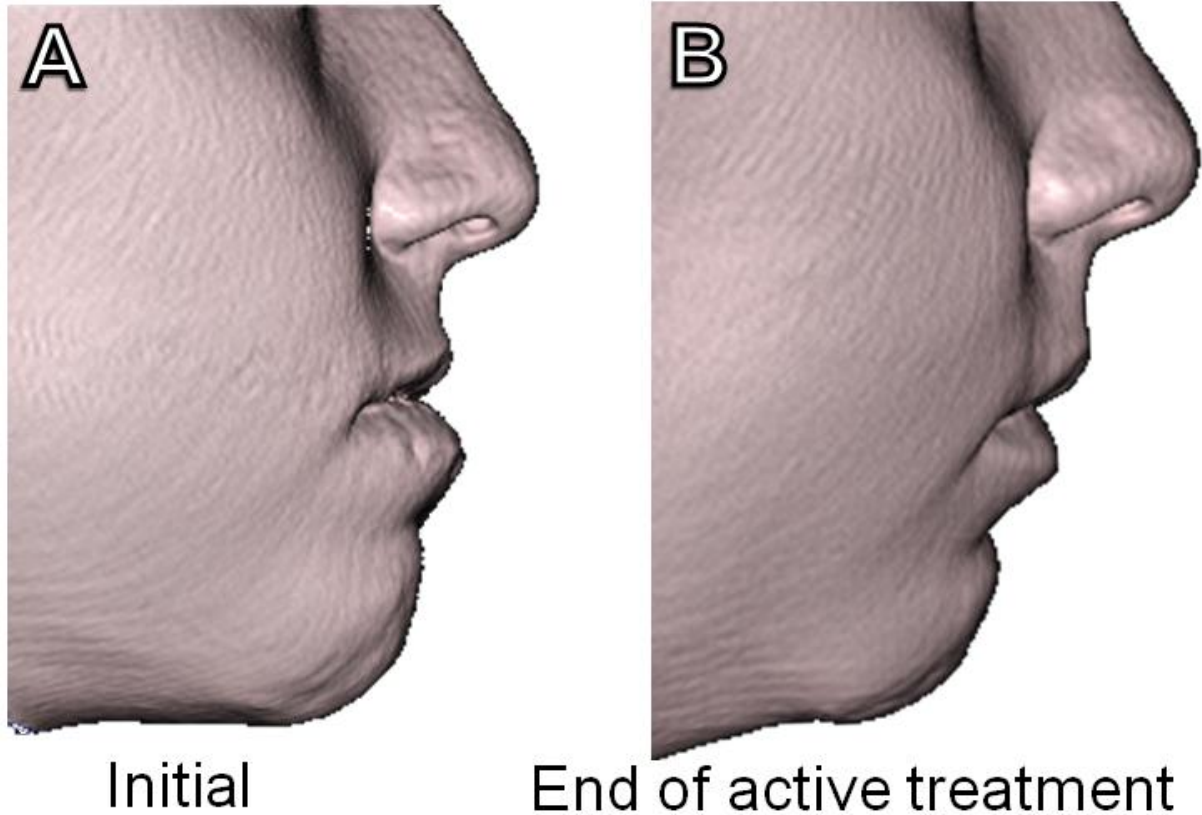


Figure 6. Boxplots of mean linear changes from T1 to T2.

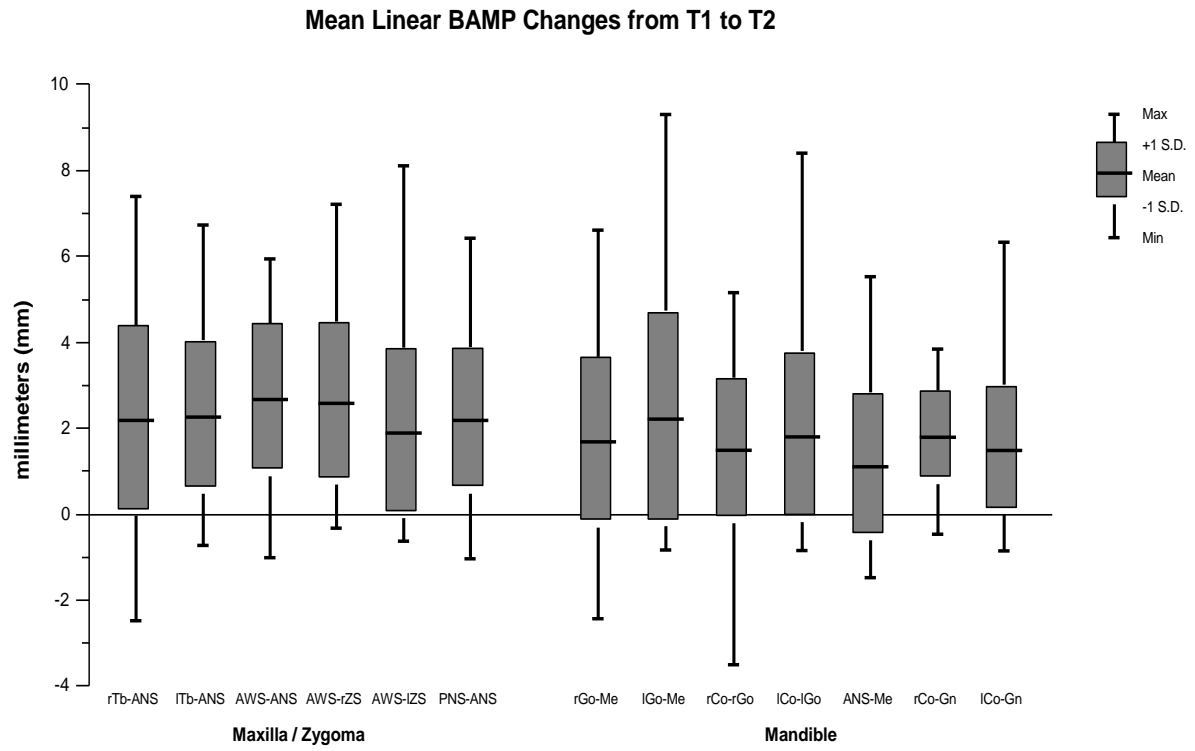


Figure 7. Boxplots of mean angular changes from T1 to T2.

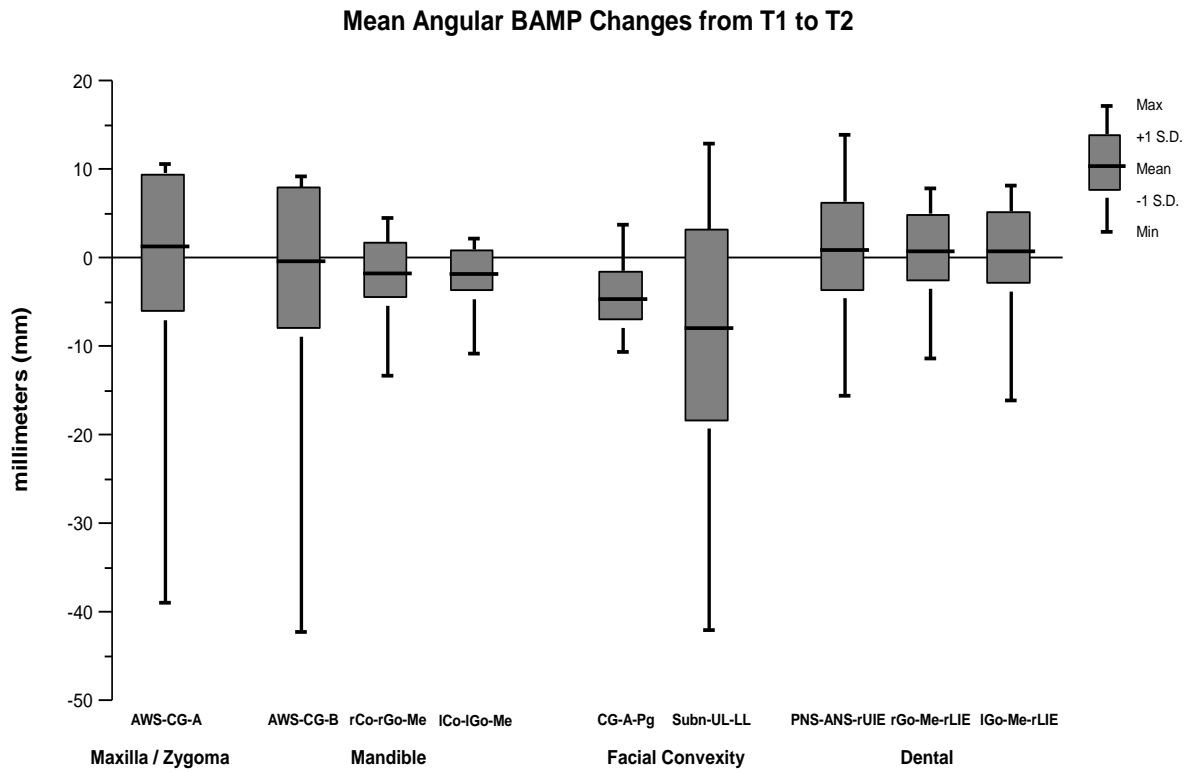
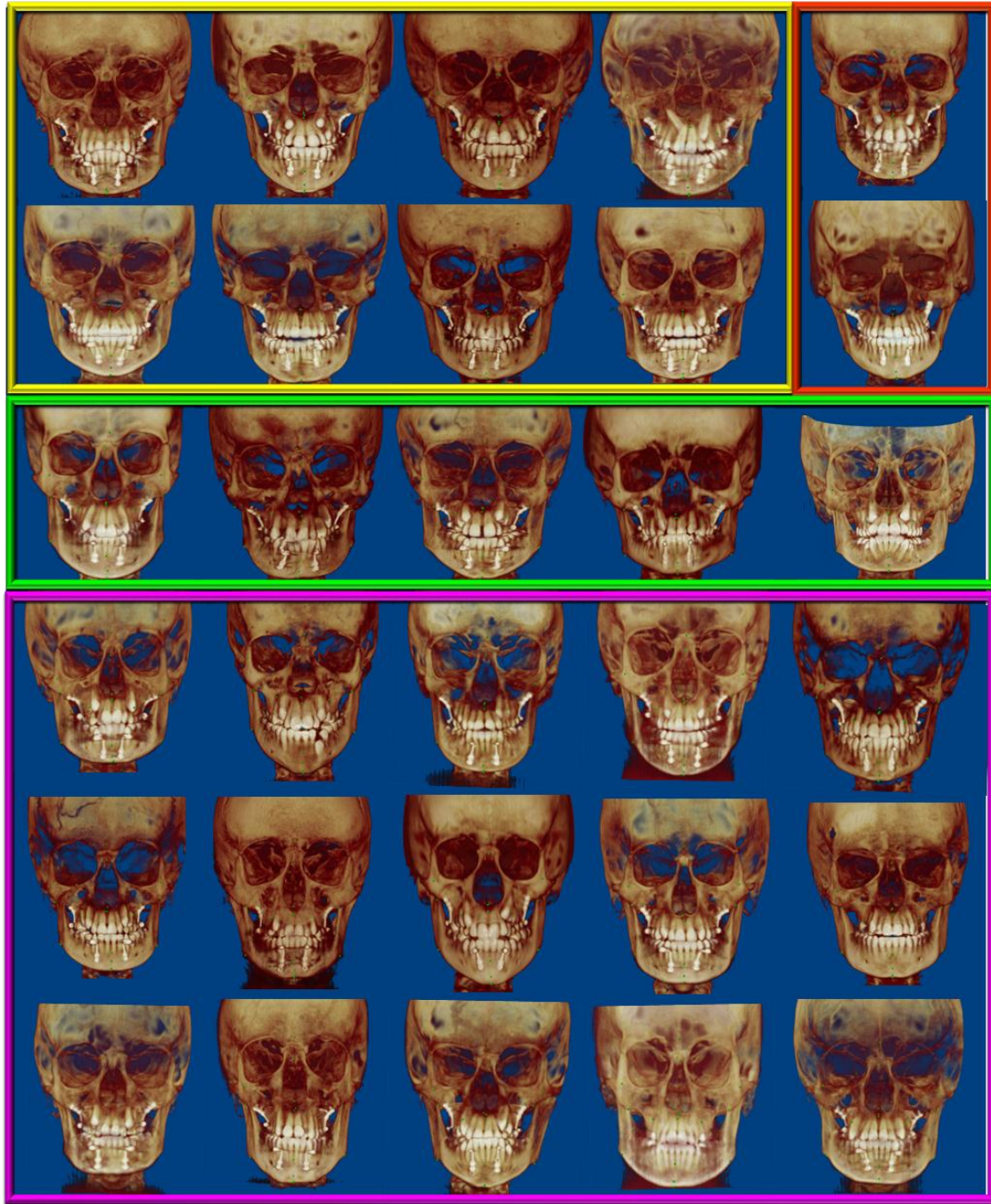


Figure 8. Exploratory subgroups (clusters) of individual variability in facial morphology as determined by the 3D composite of the landmarks included in this study. Each color box represents one of the 4 subgroups identified. Note that the subgroup in the orange box has only 2 subjects, while one group is much larger with 15 subjects. For the 3D rendering screenshots capture, head posture was standardized for all subjects.



REFERENCES

1. Proffit WR, Fields HW, Moray LJ. Prevalence of malocclusion and orthodontic treatment need in the United States: estimates from the NHANES III survey. *The International journal of adult orthodontics and orthognathic surgery*. 1998 1998/;13(2):97-106.
2. Ngan P, Yiu C, Hu A, Hägg U, Wei SH, Gunel E. Cephalometric and occlusal changes following maxillary expansion and protraction. *European journal of orthodontics*. 1998 1998/Jun;20(3):237-54.
3. Ellis E, McNamara JA. Components of adult Class III malocclusion. *Journal of oral and maxillofacial surgery: official journal of the American Association of Oral and Maxillofacial Surgeons*. 1984 1984/May;42(5):295-305.
4. Chong YH, Ive JC, Artun J. Changes following the use of protraction headgear for early correction of Class III malocclusion. *The Angle orthodontist*. 1996 1996/;66(5):351-62.
5. Gallagher RW, Miranda F, Buschang PH. Maxillary protraction: treatment and posttreatment effects. *American journal of orthodontics and dentofacial orthopedics : official publication of the American Association of Orthodontists, its constituent societies, and the American Board of Orthodontics*. 1998 1998/Jun;113(6):612-9..
6. Turley PK. Managing the developing Class III malocclusion with palatal expansion and facemask therapy. *American journal of orthodontics and dentofacial orthopedics : official publication of the American Association of Orthodontists, its constituent societies, and the American Board of Orthodontics*. 2002 2002/Oct;122(4):349-52.
7. Baccetti T, Franchi L, McNamara JA. Treatment and posttreatment craniofacial changes after rapid maxillary expansion and facemask therapy. *American journal of orthodontics and dentofacial orthopedics : official publication of the American Association of Orthodontists, its constituent societies, and the American Board of Orthodontics*. 2000 2000/Oct;118(4):404-13..
8. Gallagher RW, Miranda F, Buschang PH. Maxillary protraction: treatment and posttreatment effects. *American journal of orthodontics and dentofacial orthopedics : official publication of the American Association of Orthodontists, its constituent societies, and the American Board of Orthodontics*. 1998 1998/Jun;113(6):612-9.
9. Baccetti T, Franchi L, McNamara JA. Cephalometric variables predicting the long-term success or failure of combined rapid maxillary expansion and facial mask therapy. *American journal of orthodontics and dentofacial orthopedics : official publication of the American Association of Orthodontists, its constituent societies, and the American Board of Orthodontics*. 2004 2004/Jul;126(1):16-22.

10. Wells AP, Sarver DM, Proffit WR. Long-term efficacy of reverse pull headgear therapy. *The Angle orthodontist*. 2006 2006/Nov;76(6):915-22.
11. Westwood PV, McNamara JA, Baccetti T, Franchi L, Sarver DM. Long-term effects of Class III treatment with rapid maxillary expansion and facemask therapy followed by fixed appliances. *American journal of orthodontics and dentofacial orthopedics : official publication of the American Association of Orthodontists, its constituent societies, and the American Board of Orthodontics*. 2003 2003/Mar;123(3):306-20.
12. Delaire J. Maxillary development revisited: relevance to the orthopaedic treatment of Class III malocclusions. *European journal of orthodontics*. 1997 1997/Jun;19(3):289-311.
13. Alexander AEZ, McNamara JA, Franchi L, Baccetti T. Semilongitudinal cephalometric study of craniofacial growth in untreated Class III malocclusion. *American journal of orthodontics and dentofacial orthopedics : official publication of the American Association of Orthodontists, its constituent societies, and the American Board of Orthodontics*. 2009 2009/Jun;135(6):700.e1,14; discussion 700-1.
14. Ochoa BK, Nanda RS. Comparison of maxillary and mandibular growth. *American journal of orthodontics and dentofacial orthopedics : official publication of the American Association of Orthodontists, its constituent societies, and the American Board of Orthodontics*. 2004 2004/Feb;125(2):148-59.
15. Proffit WR, Fields HW, Sarver DM. *Contemporary orthodontics*. Anonymous Mosby St Louis, Mo; 2000.
16. Franchi L, Baccetti T, McNamara JA. Postpubertal assessment of treatment timing for maxillary expansion and protraction therapy followed by fixed appliances. *American journal of orthodontics and dentofacial orthopedics*. 2004;126(5):555-68.
17. Kapust AJ, Sinclair PM, Turley PK. Cephalometric effects of face mask/expansion therapy in Class III children: a comparison of three age groups. *American journal of orthodontics and dentofacial orthopedics : official publication of the American Association of Orthodontists, its constituent societies, and the American Board of Orthodontics*. 1998 1998/Feb;113(2):204-12.
18. Saadia M, Torres E. Sagittal changes after maxillary protraction with expansion in class III patients in the primary, mixed, and late mixed dentitions: a longitudinal retrospective study. *American journal of orthodontics and dentofacial orthopedics : official publication of the American Association of Orthodontists, its constituent societies, and the American Board of Orthodontics*. 2000 2000/Jun;117(6):669-80.
19. Merwin D, Ngan P, Hagg U, Yiu C, Wei SH. Timing for effective application of anteriorly directed orthopedic force to the maxilla. *American journal of orthodontics and*

dentofacial orthopedics : official publication of the American Association of Orthodontists, its constituent societies, and the American Board of Orthodontics. 1997
1997/Sep;112(3):292-9.

20. Takada K, Petdachai S, Sakuda M. Changes in dentofacial morphology in skeletal Class III children treated by a modified maxillary protraction headgear and a chin cup: a longitudinal cephalometric appraisal. *European journal of orthodontics*. 1993
1993/Jun;15(3):211-21

21. Cha K. Skeletal changes of maxillary protraction in patients exhibiting skeletal class III malocclusion: a comparison of three skeletal maturation groups. *The Angle orthodontist*. 2003 2003/Feb;73(1):26-35.

22. Baik HS. Clinical results of the maxillary protraction in Korean children. *American journal of orthodontics and dentofacial orthopedics : official publication of the American Association of Orthodontists, its constituent societies, and the American Board of Orthodontics*. 1995 1995/Dec;108(6):583-92.

23. Chung K, Kim Y, Linton JL, Lee Y. The miniplate with tube for skeletal anchorage. *Journal of clinical orthodontics : JCO*. 2002 2002/Jul;36(7):407-12.

24. Cornelis MA, Scheffler NR, De Clerck HJ, Tulloch JFC, Behets CN. Systematic review of the experimental use of temporary skeletal anchorage devices in orthodontics. *American journal of orthodontics and dentofacial orthopedics : official publication of the American Association of Orthodontists, its constituent societies, and the American Board of Orthodontics*. 2007 2007/Apr;131(4 Suppl):S52-8.

25. De Clerck H, Geerinckx V, Siciliano S. The Zygoma Anchorage System. *Journal of clinical orthodontics : JCO*. 2002 2002/Aug;36(8):455-9.

26. Sherwood KH, Burch J, Thompson W. Intrusion of supererupted molars with titanium miniplate anchorage. *The Angle orthodontist*. 2003 2003/Oct;73(5):597-601.

27. De Clerck HJ, Cornelis MA, Cevdanes LH, Heymann GC, Tulloch CJF. Orthopedic traction of the maxilla with miniplates: a new perspective for treatment of midface deficiency. *Journal of oral and maxillofacial surgery : official journal of the American Association of Oral and Maxillofacial Surgeons*. 2009 2009/Oct;67(10):2123-9.

28. De Clerck EEB, Swennen GRJ. Success rate of miniplate anchorage for bone anchored maxillary protraction. *The Angle orthodontist*. 2011 2011/Nov;81(6):1010-3.

29. De Clerck H, Cevdanes L, Baccetti T. Dentofacial effects of bone-anchored maxillary protraction: a controlled study of consecutively treated Class III patients. *American Journal of Orthodontics and Dentofacial Orthopedics*. 2010;138(5):577-81.

30. Baccetti T, De Clerck HJ, Cevidanes LH, Franchi L. Morphometric analysis of treatment effects of bone-anchored maxillary protraction in growing Class III patients. *European journal of orthodontics*. 2011 2011/Apr;33(2):121-5.
31. Cevidanes L, Baccetti T, Franchi L, McNamara Jr JA, De Clerck H. Comparison of two protocols for maxillary protraction: bone anchors versus face mask with rapid maxillary expansion. *Angle Orthod*. 2010;80(5):799-806.
32. Ludlow JB, Davies-Ludlow LE, Brooks SL, Howerton WB. Dosimetry of 3 CBCT devices for oral and maxillofacial radiology: CB Mercuray, NewTom 3G and i-CAT. *Dento maxillo facial radiology*. 2006 2006/Jul;35(4):219-26.
33. Hatcher DC, Aboudara CL. Diagnosis goes digital. *American journal of orthodontics and dentofacial orthopedics : official publication of the American Association of Orthodontists, its constituent societies, and the American Board of Orthodontics*. 2004 2004/Apr;125(4):512-5.
34. Mah J, Hatcher D. Three-dimensional craniofacial imaging. *American journal of orthodontics and dentofacial orthopedics : official publication of the American Association of Orthodontists, its constituent societies, and the American Board of Orthodontics*. 2004 2004/Sep;126(3):308-9.
35. Adams GL, Gansky SA, Miller AJ, Harrell WE, Hatcher DC. Comparison between traditional 2-dimensional cephalometry and a 3-dimensional approach on human dry skulls. *American journal of orthodontics and dentofacial orthopedics : official publication of the American Association of Orthodontists, its constituent societies, and the American Board of Orthodontics*. 2004 2004/Oct;126(4):397-409.
36. Kumar V, Ludlow JB, Mol A, Cevidanes L. Comparison of conventional and cone beam CT synthesized cephalograms. *Dento maxillo facial radiology*. 2007 2007/Jul;36(5):263-9.
37. de Oliveira AEF, Cevidanes LHS, Phillips C, Motta A, Burke B, Tyndall D. Observer reliability of three-dimensional cephalometric landmark identification on cone-beam computerized tomography. *Oral surgery, oral medicine, oral pathology, oral radiology, and endodontics*. 2009 2009/Feb;107(2):256-65.
38. Kaygisiz E, Tuncer BB, Yüksel S, Tuncer C, Yildiz C. Effects of maxillary protraction and fixed appliance therapy on the pharyngeal airway. *The Angle orthodontist*. 2009 2009/Jul;79(4):660-7.
39. Aboudara C, Nielsen I, Huang JC, Maki K, Miller AJ, Hatcher D. Comparison of airway space with conventional lateral headfilms and 3-dimensional reconstruction from cone-beam computed tomography. *American journal of orthodontics and dentofacial orthopedics : official publication of the American Association of Orthodontists, its constituent societies, and the American Board of Orthodontics*. 2009 2009/Apr;135(4):468-79.

40. Aboudara CA, Hatcher D, Nielsen IL, Miller A. A three-dimensional evaluation of the upper airway in adolescents. *Orthodontics & craniofacial research*. 2003 2003/;6 Suppl 1:173-5.
41. Guijarro-Martínez R, Swennen GRJ. Cone-beam computerized tomography imaging and analysis of the upper airway: a systematic review of the literature. *International journal of oral and maxillofacial surgery*. 2011 2011/Jul.
42. Iwasaki T, Hayasaki H, Takemoto Y, Kanomi R, Yamasaki Y. Oropharyngeal airway in children with Class III malocclusion evaluated by cone-beam computed tomography. *American journal of orthodontics and dentofacial orthopedics : official publication of the American Association of Orthodontists, its constituent societies, and the American Board of Orthodontics*. 2009 2009/Sep;136(3):318.e1,9; discussion 318-9.
43. Grauer D, Cevdanes LSH, Styner MA, Ackerman JL, Proffit WR. Pharyngeal airway volume and shape from cone-beam computed tomography: relationship to facial morphology. *American journal of orthodontics and dentofacial orthopedics : official publication of the American Association of Orthodontists, its constituent societies, and the American Board of Orthodontics*. 2009 2009/Dec;136(6):805-14.
44. Lenza M, Lenza MMO, Dalstra M, Melsen B, Cattaneo P. An analysis of different approaches to the assessment of upper airway morphology: a CBCT study. *Orthodontics & Craniofacial Research*. 2010;13(2):96-105.
45. Kim YJ, Hong JS, Hwang YI, Park YH. Three-dimensional analysis of pharyngeal airway in preadolescent children with different anteroposterior skeletal patterns. *American Journal of Orthodontics and Dentofacial Orthopedics*. 2010;137(3):306. e1,306. e11.
46. Lenza M, Lenza MMO, Dalstra M, Melsen B, Cattaneo P. An analysis of different approaches to the assessment of upper airway morphology: a CBCT study. *Orthodontics & Craniofacial Research*. 2010;13(2):96-105.
47. Chen L, Chen R, Yang Y, Ji G, Shen G. The effects of maxillary protraction and its long-term stability--a clinical trial in Chinese adolescents. *European journal of orthodontics*. 2011 2011/Feb.
48. Chong YH, Ive JC, Artun J. Changes following the use of protraction headgear for early correction of Class III malocclusion. *The Angle orthodontist*. 1996 1996/;66(5):351-62.
49. Yoshida I, Ishii H, Yamaguchi N, Mizoguchi I. Maxillary protraction and chin cap appliance treatment effects and long-term changes in skeletal class III patients. *The Angle orthodontist*. 1999 1999/Dec;69(6):543-52.
50. Wells AP, Sarver DM, Proffit WR. Long-term efficacy of reverse pull headgear therapy. *The Angle orthodontist*. 2006 2006/Nov;76(6):915-22.

51. Ishii H, Morita S, Takeuchi Y, Nakamura S. Treatment effect of combined maxillary protraction and chin cap appliance in severe skeletal Class III cases. *American journal of orthodontics and dentofacial orthopedics : official publication of the American Association of Orthodontists, its constituent societies, and the American Board of Orthodontics*. 1987 1987/Oct;92(4):304-12.
52. Cornelis MA, Scheffler NR, Mahy P, Siciliano S, De Clerck HJ, Tulloch JFC. Modified miniplates for temporary skeletal anchorage in orthodontics: placement and removal surgeries. *Journal of oral and maxillofacial surgery : official journal of the American Association of Oral and Maxillofacial Surgeons*. 2008 2008/Jul;66(7):1439-45.
53. De Clerck HJ, Cornelis MA, Cevidanes LH, Heymann GC, Tulloch CJF. Orthopedic traction of the maxilla with miniplates: a new perspective for treatment of midface deficiency. *Journal of oral and maxillofacial surgery : official journal of the American Association of Oral and Maxillofacial Surgeons*. 2009 2009/Oct;67(10):2123-9.
54. De Clerck H, Cevidanes L, Baccetti T. Dentofacial effects of bone-anchored maxillary protraction: a controlled study of consecutively treated Class III patients. *American journal of orthodontics and dentofacial orthopedics : official publication of the American Association of Orthodontists, its constituent societies, and the American Board of Orthodontics*. 2010 2010/Nov;138(5):577-81.
55. Heymann GC, Cevidanes L, Cornelis M, De Clerck HJ, Tulloch JFC. Three-dimensional analysis of maxillary protraction with intermaxillary elastics to miniplates. *American journal of orthodontics and dentofacial orthopedics : official publication of the American Association of Orthodontists, its constituent societies, and the American Board of Orthodontics*. 2010 2010/Feb;137(2):274-84.
56. Cevidanes L, Baccetti T, Franchi L, McNamara JA, De Clerck H. Comparison of two protocols for maxillary protraction: bone anchors versus face mask with rapid maxillary expansion. *The Angle orthodontist*. 2010 2010/Sep;80(5):799-806.
57. Nguyen T, Cevidanes L, Cornelis MA, Heymann G, de Paula LK, De Clerck H. Three-dimensional assessment of maxillary changes associated with bone anchored maxillary protraction. *American journal of orthodontics and dentofacial orthopedics : official publication of the American Association of Orthodontists, its constituent societies, and the American Board of Orthodontics*. 2011 2011/Dec;140(6):790-8.
58. Heymann GC, Cevidanes L, Cornelis M, De Clerck HJ, Tulloch JFC. Three-dimensional analysis of maxillary protraction with intermaxillary elastics to miniplates. *American journal of orthodontics and dentofacial orthopedics : official publication of the American Association of Orthodontists, its constituent societies, and the American Board of Orthodontics*. 2010 2010/Feb;137(2):274-84.

59. De Clerck H, Nguyen T, de Paula L, Cevidanes L. Mandibular and glenoid fossa changes in 3D following bone anchored Class III inter-maxillary traction. *American Journal of Orthodontics and Dentofacial Orthopedics*. Accepted Jan 2012.
60. Moyers RE, Bookstein FL. The inappropriateness of conventional cephalometrics. *American journal of orthodontics*. 1979 1979/Jun;75(6):599-617.
61. Ludlow JB, Gubler M, Cevidanes L, Mol A. Precision of cephalometric landmark identification: cone-beam computed tomography vs conventional cephalometric views. *American journal of orthodontics and dentofacial orthopedics : official publication of the American Association of Orthodontists, its constituent societies, and the American Board of Orthodontics*. 2009 2009/Sep;136(3):312.e1,10; discussion 312-3.
62. de Oliveira AEF, Cevidanes LHS, Phillips C, Motta A, Burke B, Tyndall D. Observer reliability of three-dimensional cephalometric landmark identification on cone-beam computerized tomography. *Oral surgery, oral medicine, oral pathology, oral radiology, and endodontics*. 2009 2009/Feb;107(2):256-65.
63. Ludlow JB, Gubler M, Cevidanes L, Mol A. Precision of cephalometric landmark identification: cone-beam computed tomography vs conventional cephalometric views. *American journal of orthodontics and dentofacial orthopedics : official publication of the American Association of Orthodontists, its constituent societies, and the American Board of Orthodontics*. 2009 2009/Sep;136(3):312.e1,10; discussion 312-3.
64. Baccetti T, Franchi L, McNamara JA. In: Anonymous The cervical vertebral maturation (CVM) method for the assessment of optimal treatment timing in dentofacial orthopedics. *Seminars in Orthodontics*; Elsevier; 2005. p. 119-29.
65. Kunieda E, Oku Y, Fukada J, Kawaguchi O, Shiba H, Takeda A, et al. The reproducibility of a HeadFix relocatable fixation system: analysis using the stereotactic coordinates of bilateral incus and the top of the crista galli obtained from a serial CT scan. *Phys Med Biol*. 2009;54:N197.
66. Ward Jr JH. Hierarchical grouping to optimize an objective function. *Journal of the American statistical association*. 1963:236-44.
67. Cevidanes LHC, Oliveira AEF, Grauer D, Styner M. In: Anonymous Clinical Application of 3D Imaging for Assessment of Treatment Outcomes. *Seminars in Orthodontics*; Elsevier; 2011. p. 72-80.
68. Abdelnaby YL, Nassar EA. Chin cup effects using two different force magnitudes in the management of Class III malocclusions. *Angle Orthod*. 2010;80(5):957-62.